

# Origin of magnetostriction in Fe-Ga

**Mudivarthi, Chaitanya; Laver, Mark; Cullen, James; Flatau, Alison B.; Wuttig, Manfred**

*Published in:*
Journal of Applied Physics

*Link to article, DOI:*
10.1063/1.3359814

*Publication date:*
2010

*Document Version*
Publisher's PDF, also known as Version of record

# Origin of magnetostriction in Fe–Ga

Chaitanya Mudivarthi,[1,2,a)] Mark Laver,[2,3,b)] James Cullen,[1,c)] Alison B. Flatau,[4,d)] and Manfred Wuttig[1,e)]
[1]*Materials Science and Engineering, University of Maryland, College Park, Maryland 20742, USA*
[2]*Laboratory for Neutron Scattering, Paul Scherrer Institut, 5232 Villigen PSI, Switzerland*
[3]*Materials Research Division, Risø DTU, Technical University of Denmark, DK-4000 Roskilde, Denmark*
[4]*Aerospace Engineering, University of Maryland, College Park, Maryland 20742, USA*

(Presented 19 January 2010; received 31 October 2009; accepted 4 December 2009; published online 14 May 2010)

This paper investigates the origin of large magnetostriction in Fe–Ga alloys using small-angle neutron scattering (SANS) and Kerr microscopy. The SANS data for a single-crystal, electron irradiated, and quenched $Fe_{81}Ga_{19}$ sample under externally applied magnetic and elastic fields revealed the existence of magnetostrictive nanoclusters spaced at ~15 nm apart that have a different magnetization than the A2 matrix. Combining the SANS results and the magnetization orientation obtained from the magnetic domain images using a Kerr microscope, it appears that the nanoclusters contribute significantly to the macroscopic magnetostriction. © *2010 American Institute of Physics*. [doi:10.1063/1.3359814]

Magnetostrictive materials show dimensional (magnetostriction λ) and magnetization ($M$) changes in response to magnetic or elastic fields. There is considerable interest in $Fe_{100-x}Ga_x$ alloys due to their large magnetostriction ($\lambda_{max} \sim 400\mu\varepsilon$).[1–5] Alternative magnetostrictive materials like Terfenol-D offer magnetostriction of $\sim 1800\mu\varepsilon$ but are brittle and cannot support tensile loads. Fe–Ga alloys, however, show ductilelike behavior with tensile strengths of ~500 MPa. They promise to be robust transduction materials due to their large magnetostriction, small anisotropy,[6] machinability, and low saturation fields.

The magnetostriction $(3/2)\lambda_{100}$ or $\lambda_{max}$ of single crystal $\alpha$-Fe is enhanced from $36\mu\varepsilon$ to $400\mu\varepsilon$ with the addition of the nonmagnetic element Ga. The $\lambda_{max}$ of slow-cooled $Fe_{100-x}Ga_x$ increases monotonically up to x=18 at. %. It is known that below x=18 the alloy exists in an A2 (disordered bcc) phase. Beyond x=18, a different phase ($D0_3$) precipitates in the A2 phase, degrading the magnetostriction. Quenching the samples delays the onset of $D0_3$ precipitation to x=20, thereby extending the monotonic increase in the magnetostriction to $400\mu\varepsilon$.[4] It is of high importance, scientifically and technologically, to determine the origin of this large magnetostriction enhancement.

Two possibilities for the origin of the huge increase in $\lambda_{max}$ have been offered. On one hand, the increase is ascribed to a lowering of the symmetry at Fe atoms with Ga near neighbors and thus a marked change in the local strain dependence of the magnetic anisotropy.[7] On the other hand, the effect is thought to be related to a tendency of Fe–Ga alloys to transform locally into the tetragonal structure ($D0_{22}$).[8] In this model, tetragonal distortions present in the cubic lattice (A2) are easily deformed in a magnetic field due to their magnetic coupling to the matrix.

Recent X-ray diffraction,[1] transmission electron microscopy,[9] and diffuse neutron scattering[10] studies found the existence of $D0_{22}$-like tetragonal nanoclusters in these alloys. However, the experimental means to establish the effect of nanoclusters on the magnetostriction enhancement in Fe–Ga is lacking. Measurements from DiffXAS (Ref. 2) on $Fe_{81}Ga_{19}$ showed the existence of ⟨100⟩ Ga–Ga pairs and a tenfold increase in the magnetostriction of the Fe–Ga atomic bond near a Ga–Ga environment.

In this work, small-angle neutron scattering (SANS) was used to study a quenched, electron irradiated single crystal $Fe_{81}Ga_{19}$ sample. In particular, neutrons that are scattered because of their interaction with magnetic spin are imaged. A contrast is produced due to a difference in the magnetization of the sample at different length scales. The results from SANS under externally applied magnetic and elastic fields suggest the existence of magnetostrictive nanoclusters. Combining SANS results with macroscopic magnetostriction measurements and magnetic domain images obtained from Kerr microscopy suggests the nanoclusters' contribution to the bulk magnetostriction to be significant.

A single crystal $Fe_{81}Ga_{19}$ ingot was grown at Materials Preparation Center, Ames, IA via the Bridgman technique. The ingot was annealed at 1000 °C for 168 h using a heating rate of 10 °C/min and was then water quenched to room temperature from 800 °C. A sample 25-mm-long, 15-mm-wide, and 1-mm-thick was cut along the ⟨100⟩ crystalline directions. The sample was then electron irradiated at a flux of 3 MeV, 100 mA at 100 °C for 100 min. The composition of the sample was measured using energy dispersive spectroscopy, which showed the average composition to be $Fe_{81}Ga_{19}$ with a compositional variation of 0.53 at. %.

SANS was performed using the NG3SANS instrument at the National Institute of Standards and Technology (NIST) Center for Neutron Research (NCNR) in Gaithersburg,

[a)]Tel.: +1-301-458-0304. Electronic mail: chaitanya.mudivarthi@gmail.com.
[b)]Tel.: +41-56-310-54-20. Electronic mail: mark.laver@psi.ch.
[c)]Tel.: +1-301-405-8566. Electronic mail: cullenj@umd.edu.
[d)]Tel.: 301-405-1131. Electronic mail: aflatau@umd.edu.
[e)]Tel.: +1-301-405-5212. Electronic mail: wuttig@umd.edu.

 

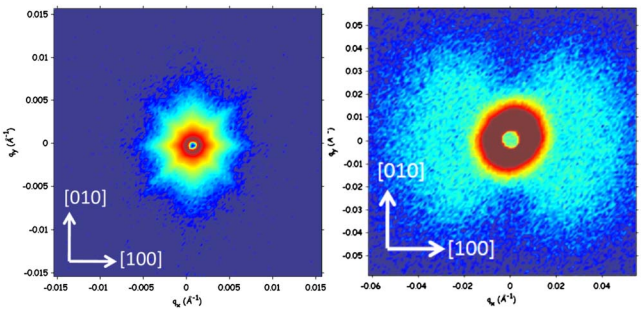


FIG. 1. (Color online) *Low q* SANS image (left) and *intermediate q* SANS image (right) at remanence.

Maryland. The sample was placed such that its long axis ([100]) is horizontal and normal to the neutron beam direction ([001]). In this work, results with unpolarized neutrons under magnetic and elastic fields are presented. Results from polarized SANS indicate negligible nuclear scattering, i.e., the scattering with unpolarized neutrons is predominantly magnetic. Detailed results of the SANS experiments with polarized and unpolarized neutrons under magnetic and elastic fields will be published elsewhere.[11]

SANS images were obtained for two configurations such that the desired scattering vector magnitude ($|q|$) range is covered. In this work, we label $|q|<0.015$ Å$^{-1}$ as *low q* and $0.015<|q|<0.05$ Å$^{-1}$ as *intermediate q*.

Figure 1 shows *low q* and *intermediate q* SANS images under no applied magnetic or elastic fields. The scattering of neutrons at *low q* is sizeable in all azimuthal directions with streaks along ⟨100⟩ and ⟨110⟩. This is expected for a homogeneous ferromagnetic material with ⟨100⟩ as the easy axis due to 90° and 180° domain walls along ⟨110⟩ and ⟨100⟩, respectively. The scattering in the *low q* range is predominantly due to the magnetic domain walls. The scattering characteristics at *intermediate q*, however, differ from a homogeneous ferromagnetic material. The scattering in this range is anisotropic with lobes along [100].

SANS under magnetic field applied along [100] shows the (i) lowering of the *low q* scattering intensity (see Fig. 2) with the applied magnetic field along both horizontal and vertical sectors, consistent with the elimination of domain walls as the magnetic field is increased. (ii) The *intermediate q* scattering intensity decreases along the horizontal sector and increases along the vertical sector, i.e., the anisotropy of the scattering rotates from [100] to [010] (see Figs. 2 and 3) direction as the field is increased to beyond saturation. The

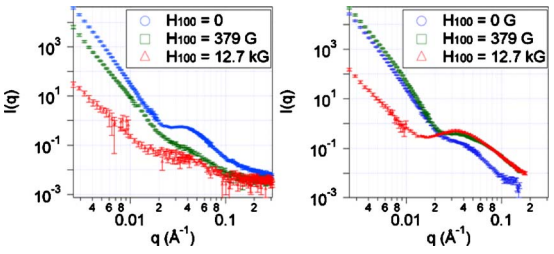


FIG. 2. (Color online) Horizontal [100] (left) and vertical [010] (right) sector averages of the SANS intensity showing the lowering of intensity in *low q* and the rotation of the SANS intensity peak in *intermediate q* from [100] to [010] as the magnetic field is increased.

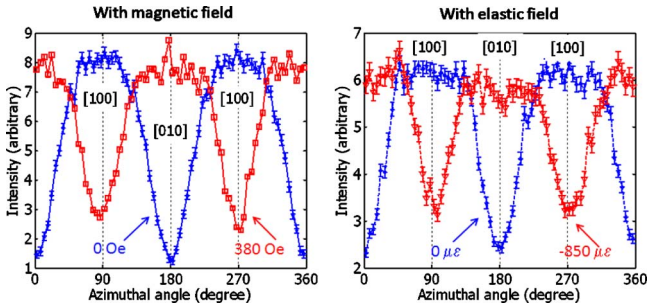


FIG. 3. (Color online) Radial (azimuthal) plot of the SANS intensity at *intermediate q* showing the rotation of the magnetization of the nanoclusters with applied magnetic field (left) and elastic field (right).

scattering intensity versus $q$ shows a peak at $|q|=0.04$ Å$^{-1}$ (see Fig. 2) corresponding to a *d*-spacing of 15 nm. The scattering sites giving rise to the intensity at *intermediate q* are hereafter termed nanoclusters.

Neutrons scatter perpendicular to the direction of the magnetic moment. So, the scattering intensity is produced only by the components of the magnetization perpendicular to the scattering vector ($q$). As a consequence, when particles of distinct magnetization are embedded in a matrix, the SANS scattering at saturation has a sine-squared angular dependence. Our sample exhibits this sine-squared angular dependence after saturation, indicating the magnetization of the nanoclusters is indeed different from the bulk. Figure 3 also shows that the scattering also has sine-squared angular dependence even when no magnetic or elastic fields were applied. Therefore, we can say that the magnetization of the nanoclusters under zero magnetic and elastic fields is predominantly along the [010] direction (perpendicular to the scattering direction). This could be either due to a remanent magnetic state or built-in residual stress. As the magnetic field along [100] is increased, the magnetization of the nanoclusters rotates from [010] to [100] resulting in the rotation of scattering intensity from [100] to [010]. As a result, the increase in the *intermediate q* SANS intensity along [010] with the magnetic field corresponds to the rotation of the magnetization of the nanoclusters.

A fixture was designed to apply an elastic field to the sample. Two resistive strain gages were bonded to the sample to measure the applied elastic field along the [100] and [010] directions, respectively. A compressive strain field from $0\mu\varepsilon$ to $1500\mu\varepsilon$ was applied along the vertical ([010]) direction.

The *intermediate q* SANS intensity under elastic field shows an identical behavior as in the case of applied magnetic field. The anisotropy of the scattering rotates from [100] and remains along [010] beyond an applied elastic field of $-800\mu\varepsilon$ (see Fig. 3), i.e., the magnetization of the nanoclusters rotates from [010] to [100] under a compressive elastic field along [010].

The magnetic domain patterns that are reported for single-crystal Fe–Ga[12] were mazelike with curvy domain walls, which contradict the expected straight 90° and 180° domain walls. In another work,[13] using magnetic force and Kerr microscopes, we show that mazelike domain patterns appear due to insufficient polishing, and when polished the

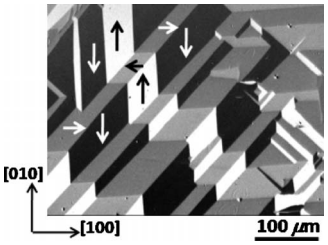


FIG. 4. Typical Kerr image on the (001) surface showing domains with in-plane magnetization and 90° and 180° domain walls.

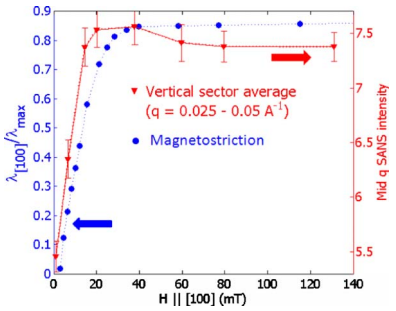


FIG. 5. (Color online) SANS *intermediate q* intensity along the vertical sector and the bulk magnetostriction as a function of applied magnetic field.

right way, the "true" domains appear. Here, we used Kerr microscope with longitudinal sensitivity and oblique incidence to image the magnetic domains. A typical Kerr image of our sample is shown in Fig. 4. The 90° and 180° domain walls are consistent with the *low q* SANS results, which showed streaks along ⟨100⟩ and ⟨110⟩. The magnetic domain images were obtained covering 14 $mm^2$ of the sample area and it was found that there is an equal distribution of the domains oriented along [100] and [010].

The SANS results indicate that (i) the magnetization of the nanoclusters exhibits a remanance, and lies predominantly along [010] under zero magnetic or elastic fields. (ii) The magnetization of the nanoclusters responds identically to the magnetic and elastic fields. Therefore, if the nanoclusters are the source of magnetostriction, one should measure 100% of the $\lambda_{max}$ instead of the expected $\lambda_{100}=2/3\lambda_{max}$ along [100].

The Kerr microscopy results indicate that the magnetization distribution of the domains is equal along the [100] and [010] directions. Therefore, if the bulk domains are the source of magnetostriction, one should measure either $2/3\lambda_{max}$ (if the domains are also equally distributed along [001]) or $1/2\lambda_{max}$. Either way, one should not measure magnetostriction more than $2/3\lambda_{max}$.

Figure 5 shows the bulk magnetostriction measurement, which shows close to 90% $\lambda_{max}$ measured along [100]. In addition, the *intermediate q* SANS intensity along the vertical sector, which provides a measure of the magnetization rotation of the nanoclusters, has a similar form to the bulk magnetostriction measurement. Therefore, the nanoclusters' contribution to the bulk magnetostriction must be significant.

In conclusion, we showed, using SANS, that nanoclusters exist in $Fe_{81}Ga_{19}$ that have a different magnetization compared with the A2 matrix in which they are embedded. The magnetization of the nanoclusters responds identically to the applied magnetic and elastic fields. Under no applied magnetic and elastic fields, the magnetization of the nanoclusters was observed to be predominantly oriented along [010]. Magnetic domain images obtained from Kerr microscope indicated that the magnetization distribution of the bulk is equal along [100] and [010]. Since the bulk magnetostriction measured was 90% of $\lambda_{max}$ along [100], it is inferred that nanoclusters contribute significantly to the bulk magnetostriction and may be crucial for the large magnetostriction enhancement in Fe–Ga alloys.

The authors would like to acknowledge the support of the U.S. Office of Naval Research and National Science Foundation in funding this research through MURI (Grant No. N000140610530) and NSF (Grant No. DMR-0705368), respectively.

[1]Q. Xing, Y. Du, R. J. McQueeney, and T. A. Lograsso, Acta Mater. **56**, 4536 (2008).
[2]M. P. Ruffoni, S. Pascarelli, R. Grossinger, R. S. Turtelli, C. Bormio-Nunes, and R. F. Pettifer, Phys. Rev. Lett. **101**, 147202 (2008).
[3]S. Pascarelli, M. P. Ruffoni, R. S. Turtelli, F. Kubel, and R. Grossinger, Phys. Rev. B **77**, 184406 (2008).
[4]A. E. Clark, K. B. Hathaway, M. Wun-Fogle, J. B. Restorff, T. A. Lograsso, V. M. Keppens, G. Petculescu, and R. A. Taylor, J. Appl. Phys. **93**, 8621 (2003).
[5]A. E. Clark, J. B. Restorff, M. Wun-Fogle, T. A. Lograsso, and D. L. Schlagel, IEEE Trans. Magn. **36**, 3238 (2000).
[6]S. Rafique, J. R. Cullen, M. Wuttig, and J. Cui, J. Appl. Phys. **95**, 6939 (2004).
[7]J. Cullen, P. Zhao, and M. Wuttig, J. Appl. Phys. **101**, 123922 (2007).
[8]A. G. Khachaturyan and D. Viehland, Metall. Mater. Trans. A **38**, 2308 (2007).
[9]S. Bhattacharyya, J. R. Jinschek, A. Khachaturyan, H. Cao, J. F. Li, and D. Viehland, Phys. Rev. B **77**, 104107 (2008).
[10]H. Cao, P. M. Gehring, C. P. Devreugd, J. A. Rodriguez-Rivera, J. Li, and D. Viehland, Phys. Rev. Lett. **102**, 127201 (2009).
[11]M. Laver, C. Mudivarthi, J. Cullen, W. Chen, S. Watson, A. Flatau, and M. Wuttig, Phys. Rev. Lett. (under review).
[12]F. Bai, J. Li, D. Viehland, D. Wu, and T. A. Lograsso, J. Appl. Phys. **98**, 023904 (2005).
[13]C. Mudivarthi, S.-M. Na, R. Schaefer, M. Laver, M. Wuttig, and A. B. Flatau, J. Magn. Magn. Mater. **322**, 2023 (available online 25 January 2010).